

Using again the residue theorem, we obtain the relation

$$P(S_{2,r}^2) = 12 \left\{ \frac{1}{2} N^2 \exp(-6N^2 S_{2,r}^2) + \sum_l \exp(-6N^2 S_{2,r}^2 \sin^2 \gamma_l) [12N^4 S_{2,r}^2 \sin^4 \gamma_l \cos^2 \gamma_l + N^2 \sin^2 \gamma_l (4 \sin^2 \gamma_l - 3)] \right\} \quad (14)$$

differing from the corresponding function for  $N$  odd, eq 10b, only by the first term and the summation extending from one to  $N_2$ . With increasing  $N$  the first term diminishes rapidly and goes to zero for  $N \rightarrow \infty$ , as can be expected. Of course

both eq 10b and 14 should represent the same family of functions and, accordingly, they can be transcribed in the form which is independent of whether  $N$  is even or odd

$$P(S_{2,r}^2) = 6 \sum_{l=1}^{N-1} \exp(-6N^2 S_{2,r}^2 \sin^2 \gamma_l) \times [12N^4 S_{2,r}^2 \sin^4 \gamma_l \cos^2 \gamma_l + N^2 \sin^2 \gamma_l (4 \sin^2 \gamma_l - 3)] \quad (15)$$

**Acknowledgment.** The author wishes to thank Dr. W. Gobush for fruitful discussions. The work was supported by the Michigan Foundation for Advanced Research.

## Three-Dimensional Conformations of Polypeptide Chains by Monte Carlo Calculation. I. Model for Random-Coil Conformation

Seiji Tanaka and Akio Nakajima\*

Department of Polymer Chemistry, Kyoto University, Kyoto 606, Japan.

Received April 17, 1972

**ABSTRACT:** The three-dimensional conformations of polypeptide chains were studied by the Monte Carlo calculation. A simplified model was proposed for the randomly coiled conformation of poly(L-alanine). The conformations generated were classified into "allowed" and "disallowed" conformations, according to the size of the nonbonded interaction energies calculated by use of the Lennard-Jones potential function for pairs of atoms and atomic groups. The chains formed by allowed conformations are equivalent to the "non-self-intersecting chains" usually used. The mean-square end-to-end distance ( $R^2$ ) and the mean-square radius of gyration ( $S^2$ ) obtained by taking into account the long-range interaction for randomly coiled chain conformations were essentially consistent with those previously obtained by Monte Carlo calculations based on lattice and nonlattice models. Unperturbed dimensions were also calculated by two different methods. One was a Monte Carlo method in which checking of atomic overlaps was omitted, and the other an exact calculation employing conformational statistics of polymer chains. These unperturbed dimensions were compared with perturbed dimensions obtained by a non-self-intersecting chain model.

Recently statistical-mechanical treatments of polymer chain conformations have been successfully applied to the calculation of unperturbed chain dimension of polypeptides by Flory and his coworkers<sup>1-5</sup> and later by ourselves.<sup>6-8</sup> These theoretical treatments were supported by experimental results.<sup>9-11</sup> Theoretical studies have also been carried out to predict the stability of helical conformations.<sup>12-15</sup> In all the studies mentioned above calculations of conformational energy were performed on the basis of available information

on the potential of interaction between nonbonded atoms and atomic groups. The hard-sphere model<sup>16,17</sup> was useful only to classify conformations which are sterically allowed and not allowed. The energy calculation methods using semiempirical potential functions made possible evaluation of the most stable helical structure, and the stability or statistical weight of various conformations in the random-coil state. In the statistical-mechanical treatments of chain conformations and helix-coil transitions, polypeptide chains have been regarded as one-dimensional cooperative systems governed by short-range interactions. Accordingly, the conformational properties obtained there are compared with those observed experimentally in the  $\theta$  state.

Long-range interactions or excluded volume effects should play an important role in randomly coiled conformations in the nonideal state for biopolymers and their synthetic analogs, by analogy with ordinary polymers. The excluded-volume problems in polymer chains have been studied with the Monte Carlo method by a number of investigators. Wall, *et al.*,<sup>18</sup> have used a method based on the non-self-intersecting random

(1) D. A. Brant and P. J. Flory, *J. Amer. Chem. Soc.*, **87**, 663, 2791 (1965).

(2) W. G. Miller, D. A. Brant, and P. J. Flory, *J. Mol. Biol.*, **23**, 47 (1967).

(3) P. R. Schimmel and P. J. Flory, *Proc. Nat. Acad. Sci. U. S.*, **58**, 52 (1967).

(4) P. J. Flory and P. R. Schimmel, *J. Amer. Chem. Soc.*, **89**, 6807 (1967).

(5) Above works are accumulated in P. J. Flory, "Statistical Mechanics of Chain Molecules," Interscience, New York, N. Y., 1969.

(6) S. Tanaka and A. Nakajima, *Polym. J.*, **1**, 71 (1970).

(7) S. Tanaka and A. Nakajima, *ibid.*, **2**, 717 (1971).

(8) S. Tanaka and A. Nakajima, *ibid.*, **2**, 725 (1971).

(9) D. A. Brant and P. J. Flory, *J. Amer. Chem. Soc.*, **87**, 2788 (1965).

(10) S. Tanaka and A. Nakajima, *Polym. J.*, in press.

(11) A. Nakajima, S. Tanaka, and K. Itoh, *ibid.*, **3**, 398 (1972).

(12) R. A. Scott and H. A. Scheraga, *J. Chem. Phys.*, **45**, 2091 (1966).

(13) T. Ooi, R. A. Scott, G. Vanderkooi, and H. A. Scheraga, *ibid.*, **46**, 4410 (1967).

(14) D. A. Brant, *Macromolecules*, **1**, 291 (1968).

(15) S. Tanaka and A. Nakajima, *Polym. J.*, **1**, 505 (1970).

(16) G. N. Ramachandran, C. Ramakrishnan, and V. Sasisekharan, *J. Mol. Biol.*, **7**, 95 (1963).

(17) G. Némethy and H. A. Scheraga, *Biopolymers*, **3**, 155 (1965).

(18) F. T. Wall, S. Windwer, and P. J. Gans, "Methods in Computational Physics," Vol. 1, Academic Press, New York, N. Y., 1963, p 217; F. T. Wall and J. J. Erpenbeck, *J. Chem. Phys.*, **30**, 634, 637 (1959).

walks on a regular lattice. Windwer<sup>19</sup> and Loftus and Gans<sup>20</sup> have studied the problem by a nonlattice system differing from the lattice-constrained self-avoiding walks. A test of the expansion factor for polymer chains was carried out by employing self-avoiding random walks on a four-choice cubic lattice by Alexandrowicz.<sup>21</sup> Wall,<sup>18</sup> Fluendy,<sup>22</sup> and Suzuki and Nakata<sup>23</sup> have treated this problem by taking into account energy contributions. More recently, a Monte Carlo calculation for randomly coiling polypeptide chains has been performed by Knaell and Scott,<sup>24</sup> who used a hard-sphere model.

In the present paper we investigate the conformational properties of polypeptides in randomly coiled conformations by considering the excluded-volume effect with the use of a Monte Carlo method. The first purpose of this work consists of understanding the nature of random-coil conformations of the polypeptide chain model proposed by us and employed here, in particular, for poly(L-alanine). We use a realistic model, in which are included three types of interaction potential, *i.e.*, a hard-sphere potential, a nonbonded interaction potential of the Lennard-Jones type, and, in addition to the latter, an electrostatic interaction potential between dipole charges of amide groups. The second purpose of this paper is to establish a treatment for chain conformation of the randomly coiling part of partly helical molecules, *e.g.*, the chain conformations of polypeptide molecules in the region of the helix-coil transition and of protein molecules. The model employed here will be further developed in a succeeding paper<sup>25</sup> on the dimensional changes of polypeptides in the region of the helix-coil transition.

## I. Model

The polypeptide chain model employed here is essentially based on previous work.<sup>1-8,12-15</sup> A polypeptide chain in fully extended conformation is shown in Figure 1. The geometric description of the chain is in accordance with the standard convention<sup>26</sup> for polypeptides. The fixed bond angles and bond lengths used in the present calculation are the same as those employed in previous work.<sup>7,12,13</sup> The amide bonds are fixed in the rigid planar trans conformation. Rotations are allowed around the N-C $\alpha$  and C $\alpha$ -C' single bonds, which are denoted by  $\phi$  and  $\psi$ , respectively. The distance between neighboring  $\alpha$ -carbons is given by a virtual bond length of 3.8 Å, and the orientation of residue *i* is determined by the pair of rotational angles  $\phi_i$  and  $\psi_i$ .

From a fundamental point of view, the term "non-self-intersection" should not be employed when we use the Lennard-Jones potential function. We should use the term "non-self-steric-hindering chains" or "non-self-overlapping chains" rather than "non-self-intersecting chains." However, we shall hereafter use the term "non-self-intersecting chains," in accordance with conventional usage in the Monte Carlo calculation for polymer chains. The conformation which gives relatively high energy may be practically regarded as a disallowed one. In this study, therefore, when the nonbonded interaction energy for a single pair of atoms or atomic groups exceeded a gate quantity  $E_{\max}$ , we regarded that atomic over-

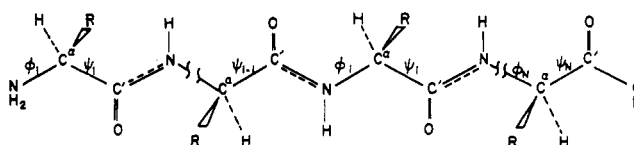


Figure 1. An  $\alpha$ -L-polypeptide chain in its extended conformation. For poly(L-alanine), the R groups are CH<sub>3</sub>.

lapping had occurred, and such a chain conformation was discarded. In the actual calculation we used the gate quantity  $E_{\max} = 6$  kcal/mol, which is rather arbitrary but high enough to give only a negligible contribution to the final averages. The chains thus obtained were termed non-self-intersecting chains in accordance with the conventional usage in Monte Carlo studies, although it was unsuitable, as mentioned above, in the present case. For the non-self-intersecting chains generated, statistical-mechanical averages of end-to-end distance and radius of gyration were calculated by means of the two following procedures. One method takes into consideration the contributions of conformational energy; the other is that usually used for the hard-sphere model. In the former case the nonbonded interaction energies are given by eq 1 for atomic pairs having greater internuclear distances than the distance  $r_{\min}^*$  at which the interaction energy goes up to  $E_{\max}$ . Further,  $E$  becomes infinite for  $r < r_{\min}^*$ ; all long-distance forces are attractive. The potential functions used in the calculation of conformational energies are described later in detail. The second procedure is similar to that for the hard-sphere model, and therefore we use the term "hard-sphere model" hereafter for convenience. In the hard-sphere model used here, the allowed and disallowed conformations are based on the contact distance  $r_{\min}^*$  instead of the sum of the van der Waals radii, and all the allowed conformations thus obtained have equal energy. In this model, the atoms and atomic groups can penetrate each other slightly within the sum of the van der Waals radii. We employ the latter procedure in this work because we can obtain effective results from a finite number of samples within a reasonable computational time and can then compare the result with previous results for non-self-intersecting chains obtained by other authors.

The interaction energies used for checking the atomic overlaps and the conformational energies of generated non-self-intersecting chains were calculated by using the semi-empirical potential functions which have been employed in previous work.<sup>1-8,12-15</sup>

In calculating the nonbonded interaction energies for the pairs of nonbonded atoms in polypeptide chains, we used the Lennard-Jones 6-12 potential function, which is of the form

$$V_{(W)jk} = d_{jk}/r_{jk}^{12} - e_{jk}/r_{jk}^6 \quad (1)$$

The coefficient  $e_{jk}$  [(kcal Å<sup>6</sup>)/mol] was calculated by the Slater-Kirkwood equation

$$e_{jk} = \frac{(3/2)e(\hbar/m^{1/2})\alpha_j\alpha_k}{(\alpha_j/N_{j,\text{eff}})^{1/2} + (\alpha_k/N_{k,\text{eff}})^{1/2}} \quad (2)$$

where  $e$  is the elementary electronic charge,  $\hbar$  Planck's constant,  $m$  the electronic mass,  $\alpha$  the atomic polarizability, and  $N_{\text{eff}}$  the effective number of electrons in the outer electronic subshell. The coefficient  $d_{jk}$  [(kcal Å<sup>12</sup>)/mol] was estimated from

$$d_{jk} = e_{jk}(r_{\min})^6/2 \quad (3)$$

- (19) S. Windwer, *J. Chem. Phys.*, **43**, 115 (1965).
- (20) E. Loftus and P. J. Gans, *ibid.*, **49**, 3828 (1968).
- (21) Z. Alexandrowicz, *ibid.*, **51**, 561 (1969).
- (22) M. A. D. Fluendy, *Trans. Faraday Soc.*, **59**, 1681 (1963).
- (23) K. Suzuki and Y. Nakata, *Bull. Chem. Soc. Jap.*, **43**, 1006 (1970).
- (24) K. K. Knaell and R. A. Scott, *J. Chem. Phys.*, **54**, 566 (1971).
- (25) S. Tanaka and A. Nakajima, *Macromolecules*, **5**, 714 (1972).
- (26) J. T. Edsall, P. J. Flory, J. C. Kendrew, A. M. Liquori, G. Némethy, G. N. Ramachandran, and H. A. Scheraga, *Biopolymers*, **4**, 121 (1966).

TABLE I  
PARAMETERS FOR CALCULATING NONBONDED  
POTENTIAL FUNCTIONS

Atom or atomic group	Polarizability $\alpha \times 10^{24}, \text{cm}^3$	$N_{\text{eff}}$	van der Waals radius, Å
H	0.42	0.9	1.20
C	1.30	5	1.70
N	1.15	6	1.55
O	0.84	7	1.50
CH <sub>3</sub>	2.17	8	1.85
NH <sub>2</sub> <sup>a</sup>	2.13	9	1.65
OH <sup>a</sup>	2.14	6	1.50

<sup>a</sup> The values for NH<sub>2</sub> and OH were assumed to be the same as those<sup>27</sup> for NH<sub>3</sub><sup>+</sup> and O<sup>-</sup> (carbonyl), respectively.

TABLE II  
PARTIAL CHARGES ON AMIDE GROUP

Atom $i$	Charge, $\delta_i$
H'	0.272
N	-0.305
C'	0.449
O	-0.416

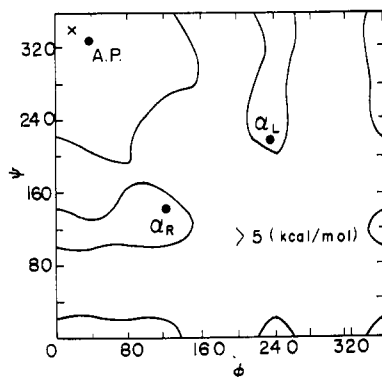


Figure 2. Conformational energy map for the alanyl dipeptide model. The regions in which conformational energies are lower than 5 kcal/mol are enclosed by solid curves. Conformational states employed in this calculation are indicated by ●;  $\alpha_R$  for the right-handed  $\alpha$  helix,  $\alpha_L$  for the left-handed  $\alpha$  helix, and A.P. for the antiparallel pleated sheet. The energy minimum is indicated by ×.

where  $r_{\min}$  denotes the atomic distance at which  $V_{(W)jk}$  is minimum. Following Miller, *et al.*,<sup>2</sup>  $r_{\min}$ 's are equal to  $r_j^0 + r_k^0 + 0.20$  (Å), where  $r_j^0$  and  $r_k^0$  are the van der Waals radii (Å) of atoms  $j$  and  $k$ , respectively. The values of the polarizability, the effective number of electrons, and the van der Waals radii used here are listed in Table I. The energy of interaction between dipole moments of amide groups was calculated by the point-monopole approximation.<sup>2</sup> The equation for the electrostatic interaction between the partial charges is

$$V_{(D)jk} = 332.0 \delta_j \delta_k / \epsilon r_{jk} \quad (4)$$

The  $\delta$  values are partial charges evaluated by Ooi, *et al.*,<sup>13</sup> and are given in Table II, and  $\epsilon$  is the effective local dielectric constant. We have used 3.5 for  $\epsilon$ , which led to theoretical results<sup>1-8</sup> on unperturbed dimensions in conformity with experimental results.<sup>9-11</sup>

TABLE III  
ALLOWED CONFORMATIONAL STATES

Conformation	$\phi$ (N-C $\alpha$ ), deg	$\psi$ (C $\alpha$ -C'), deg
Right-handed $\alpha$ helix	122	133
Left-handed $\alpha$ helix	238	227
Extended form (antiparallel pleated sheet) <sup>a</sup>	38	325

<sup>a</sup> Data from T. Miyazawa in "Poly- $\alpha$ -Amino Acids," G. D. Fasman, Ed., Marcel Dekker, New York, N. Y., 1967, Chapter 2.

The contribution of short-range interactions to chain conformations for the dipeptide model of poly(L-alanine) is understandable from the energy map of Figure 2 taken from our previous work.<sup>7</sup> This energy map was obtained by using the intrinsic threefold torsional potentials about the bonds N-C $\alpha$  and C $\alpha$ -C', and, in addition, the nonbonded and electrostatic interactions described above. There exist three low-energy regions, each having a distinct energy minimum. Numerical values obtained are given in Table III. Conformations approximately corresponding to these three energy minima were chosen as three acceptable conformations. They are the right-handed  $\alpha$ -helical conformation ( $\alpha_R$ ), the left-handed  $\alpha$ -helical conformation ( $\alpha_L$ ), and the antiparallel pleated sheet conformation. In addition, we assumed that these three conformations occur equivalently. As is seen in the energy map of alanyl dipeptide,<sup>8</sup> the low-energy region in which the antiparallel pleated sheet conformation is included contributes predominantly to the chain conformation of poly(L-alanine). If the energy difference is appropriately assigned to each of the three allowed conformations, then our three-state model yields<sup>28</sup> the same values of  $\langle R_0^2 \rangle$  and  $\langle S_0^2 \rangle$  as those calculated by the method reported previously.<sup>8</sup> It was also found<sup>28</sup> in this respect that greater chain lengths and a larger number of samples were necessary to observe the exclusion effect in the Monte Carlo calculation for non-self-intersecting chains, because the extended conformation is more stable than other conformations. Such consideration may lead to the conclusion that the calculation cannot be completed within reasonable computational time. However, it is possible to improve the model by including directly short-range interaction energy and by improving the chain generation technique, as will be performed in our future work.

## II. Computational Procedure by the Monte Carlo Method

The main part of the computer program in Monte Carlo calculations consists in the generation of non-self-intersecting chains without atomic overlap. The process begins with the determination of the conformational state for the first amino acid residue, NH<sub>2</sub>-C $\alpha$ HR-CO-, by random selection of one of three states. The conformations for the second and third residues are successively determined at random and linked to the preceding one. After the fourth unit is added in the same manner, atomic overlaps are checked according to the method described in the previous section. Thus, at every addition of an  $i$ th residue, it is necessary to check the atomic overlaps between the  $i$ th residue and all the residues preceding it except the  $(i-1)$  and  $(i-2)$  ones. This process is continued until either a non-self-intersecting chain of a desired length is completed or an atomic overlap is found. If found, such a chain conformation is discarded,

(27) K. D. Gibson and H. A. Scheraga, *Proc. Nat. Acad. Sci. U. S.*, **58**, 420 (1967).

(28) S. Tanaka and A. Nakajima, unpublished data.

and the above process is repeated from the beginning of the chain. If completed, the data on the non-self-intersecting chain are stored and atomic overlap is artificially given at the end of the chain to start a new attempt. When all the conformations for three consecutive residues are either in the right-handed  $\alpha$  helix or in the left-handed  $\alpha$  helix, we find steric hindrance between the  $C'_{i-4}-O_{i-4}$  group of the  $(i-4)$  residue and the  $N_i-H_i$  of the  $i$  residue. These conformations in polypeptides are stabilized by hydrogen bonds. In the present study we allow these conformations by regarding that the steric repulsions are compensated by hydrogen bonds without contributing to the conformational energy.

Long non-self-intersecting chains are difficult to achieve even when the walks are constrained to a regular lattice.<sup>18</sup> In the case of the realistic model employed here, the problem is much more difficult. In order to complete the calculations for long chain lengths in reasonable machine time, it is necessary to devise a computational procedure. For this purpose we have employed two major methods, "cutting off" and "chain enrichment," as described below.

We may neglect the nonbonded interactions between atoms which are far apart, since their contributions to the final results are small. Ooi, *et al.*,<sup>13</sup> have neglected nonbonded energies between atomic pairs for  $r_{jk} > 7 \text{ \AA}$  in the conformational analysis of helical structures. Before overlap checks on atomic pairs, the distance  $R$  between  $\alpha$ -carbons, which are located near the center of the amino acid residues, is evaluated as a measure of distance between the residues under consideration. If  $R$  is larger than  $R'$ , there is no overlap between the residual units, in other words, between the pairs of atoms involved in them. If  $R < R'$ , overlaps are checked for every pair of atoms involved in the residues under consideration, and nonbonded energies are calculated. Further, we compare  $R$  with  $R''$ . If  $R \leq R''$ , we calculate the electrostatic energies between amide dipoles, but cut them off in case  $R > R''$ . The distance  $R''$  must be much longer than  $R'$ , because electrostatic interactions are of longer range.  $R'$  and  $R''$  in the present calculation are 7 and 20  $\text{\AA}$ , respectively.

As the second method, we employed the chain-enrichment technique developed by Wall, *et al.*,<sup>18</sup> *i.e.*, the s,p routine technique. This technique is a powerful method for dealing with chain attrition at greater chain lengths. Without use of this enrichment technique, we were able to obtain only several chains consisting of 20 residues for 20 min with the FACOM 230-60 computer of the Kyoto University Computation Center.

### III. Results and Discussion

(A) **Attrition.** The attrition parameter  $\lambda$  is represented<sup>18</sup> by

$$W_N = W_0 \exp(-\lambda N) \quad (5)$$

where  $W_N$  is the number of chains successfully reached up to  $N$  residues, and  $W_0$  is the number of chains started. When the chain-enrichment technique proposed by Wall, *et al.*,<sup>18</sup> is used, eq 5 is modified to the following form

$$W_N = p^{i-1} W_0 \exp(-i\lambda s) \quad (6)$$

where  $i$  is the number of segments given by  $N/s$ , and  $p$  is the number of attempts to generate each segment. The attrition parameter should be obtained from the slope of a plot of  $\ln W_N$  vs.  $N$ . The above relation, however, gives a straight line only in the range of longer chain length ( $N > ca. 200$  for the tetrahedral lattice<sup>18</sup>). Therefore, in this study,  $\lambda$  values were calculated for each step by use of eq 5 and 6. The average values and standard deviation for six to ten

TABLE IV  
ATTRITION VALUES

$N$	$\lambda$	St dev
6	0.010	0.003
10	0.027	0.006
15	0.037	0.004
20	0.050	0.004
41	0.071	0.008
71	0.093	0.007
101	0.122	0.004
121	0.133	0.005
151	0.141	0.004

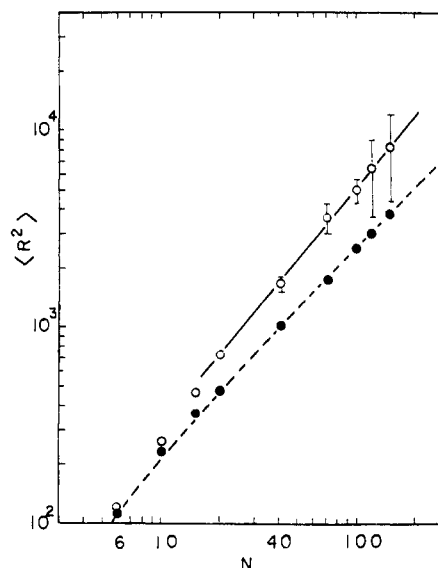


Figure 3. Plots of  $\log \langle R^2 \rangle_H$  (O),  $\log \langle R^2 \rangle^*$  (●), and  $\log \langle R^2 \rangle$  (---) against  $\log N$ . A least-squares fit of eq 9 to the data of non-self-intersecting chains for  $N \geq 20$  is shown by the solid line. Standard deviations are shown by vertical bars.

batches are given in Table IV. As is seen from Table IV,  $\lambda$  does not converge even at  $N = 151$ . Similar trends for  $\lambda$  were found by Knaell and Scott,<sup>24</sup> who obtained an asymptotic value  $\lambda_\infty = 0.13133$  for infinite chain length by extrapolation. Our value of  $\lambda$  at  $N = 151$  is larger than their value. Such a difference is due to the difference in the models used, mainly to the difference in contact distances of atomic pairs. The attrition parameter  $\lambda$  is dependent on the type of lattice.<sup>18,20</sup> It has also been found that  $\lambda$  depends on the allowed contact distance of atomic pairs.<sup>28</sup> For example, we have obtained  $\lambda = 0.037$  at  $N = 15$  for the non-self-intersecting chain model used here, while  $\lambda = 0.075$  for a different model in which the sums of the van der Waals radii were employed as the contact distances. This latter value is almost the same as that obtained by Knaell and Scott.<sup>24</sup>

(B) **Chain Dimensions.** The square of the end-to-end distance,  $r^2$ , and the square of the radius of gyration,  $s^2$ , were calculated for non-self-intersecting chains completed up to a desired chain length. For the hard-sphere model employed here, we obtained six to ten batches which consist of 100 or 50 non-self-intersecting chains. The mean-square end-to-end distance,  $\langle R^2 \rangle_H$ , and the mean-square radius of gyration,  $\langle S^2 \rangle_H$ , for the hard-sphere model were calculated by averaging over all these batch-averaged values,  $\langle r^2 \rangle$  and  $\langle s^2 \rangle$ . When the contributions of conformational energies are taken into con-

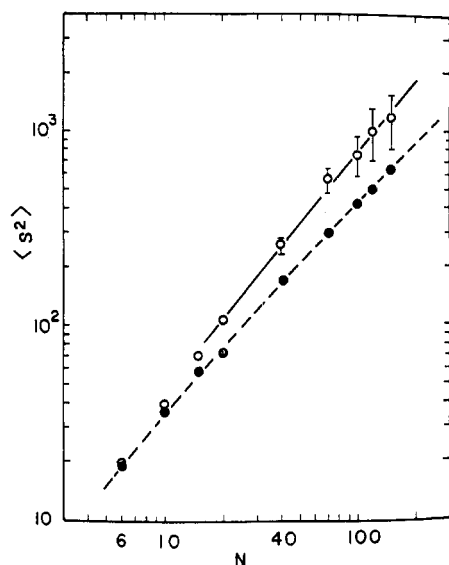


Figure 4. Plots of  $\log \langle S^2 \rangle_H$  (○),  $\log \langle S_0^2 \rangle^*$  (●), and  $\log \langle S_0^2 \rangle$  (---) against  $\log N$ . A least-squares fit of eq 10 to the data of non-self-intersecting chains for  $N \geq 20$  is shown by the solid line. Standard deviations are shown by vertical bars.

TABLE V  
PARAMETERS IN EQUATIONS  $\langle R^2 \rangle = aN^b$  AND  $\langle S^2 \rangle = lN^m$

Parameter	—Monte Carlo calculation—		Exact calculation for unperturbed chain
	Non-self-intersecting chain	Unperturbed chain	
$a$	19.548	24.247	23.379
$b$	1.2075	1.0060	1.0182
$l$	2.8153	3.8927	3.8097
$m$	1.2171	1.0145	1.0221

sideration, the average values are denoted by  $\langle R^2 \rangle_{V,D}$  and  $\langle S^2 \rangle_{V,D}$ ,  $\langle R^2 \rangle_{V,D}$  being obtained from

$$\langle R^2 \rangle_{V,D} = \frac{\sum_{j=1}^k r_j^2 \exp(-E_{V,D(j)}/RT)}{\sum_{j=1}^k \exp(-E_{V,D(j)}/RT)} \quad (7)$$

where  $k$  is the total number of non-self-intersecting chains (500–600 chains in this study) and  $E_{V,D(j)}$  is the sum of non-bonded and dipole interaction energies for a conformational state of the  $j$ th chain calculated by the method described above with  $T = 303.0^\circ\text{K}$ . The biasing factor<sup>18</sup> was excluded in eq 7, since the Monte Carlo generation was carried out in an unbiased fashion.  $\langle S^2 \rangle_{V,D}$  is obtained in a similar manner. For the case in which only the nonbonded interactions are taken into account (neglecting electrostatic interactions), these averaged values were denoted by  $\langle R^2 \rangle_V$  and  $\langle S^2 \rangle_V$ , which were obtained by substituting  $E_{V(j)}$ , i.e., conformational energies only from nonbonded interactions, for  $E_{V,D(j)}$  in eq 7. Detailed analyses for data were carried out here only for  $\langle R^2 \rangle_H$  and  $\langle S^2 \rangle_H$  for a reason to be described later.

Unperturbed chain dimensions were obtained by two different methods. One set of unperturbed chain dimensions, expressed as  $\langle R_0^2 \rangle^*$  and  $\langle S_0^2 \rangle^*$ , were obtained from a Monte Carlo calculation in which checking for atomic overlaps was not performed. The actual calculations were carried out for a finite number of chains (6 batches each consisting of

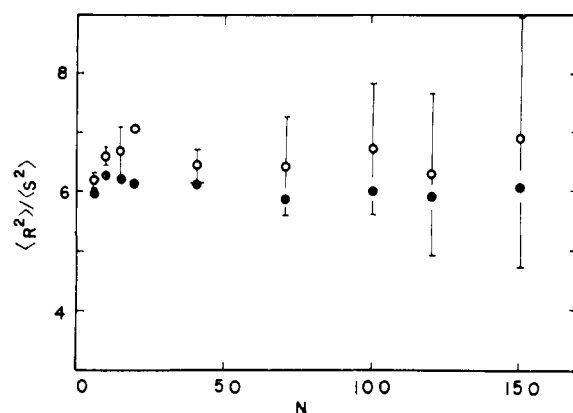


Figure 5. Plots of  $\langle R^2 \rangle_H / \langle S^2 \rangle_H$  against  $N$  (○) and  $\langle R_0^2 \rangle^* / \langle S_0^2 \rangle^*$  against  $N$  based on the data obtained directly from Monte Carlo calculations. Standard deviations are shown by vertical bars.

100 chains). The other set of unperturbed chain dimensions, expressed as  $\langle R_0^2 \rangle$  and  $\langle S_0^2 \rangle$ , was obtained from the exact calculation method by statistical-mechanical averaging over all conformations of the polymer chain in the unperturbed state.<sup>5</sup> We obtain  $\langle R_0^2 \rangle$  by replacing  $\langle T \rangle$  in eq 10 of our previous paper<sup>8</sup> with

$$\langle T_c \rangle = \begin{pmatrix} 0.232 & -0.239 & 0.202 \\ -0.080 & 0.226 & 0.074 \\ 0.215 & 0.014 & -0.357 \end{pmatrix} \quad (8)$$

Equation 8 is the averaged transformation matrix of a virtual bond<sup>8</sup> for the equivalent three-state model employed here. The exact unperturbed chain dimensions obtained by this method are denoted by  $\langle R_0^2 \rangle$  and  $\langle S_0^2 \rangle$ .

The results for  $\langle R^2 \rangle_H$ ,  $\langle R_0^2 \rangle^*$ , and  $\langle R_0^2 \rangle$  are shown in Figure 3, in which  $\log \langle R^2 \rangle_H$ ,  $\log \langle R_0^2 \rangle^*$ , and  $\log \langle R_0^2 \rangle$  are plotted against  $\log N$ . In Figure 4 the results on the mean-square radius of gyration are given in a similar manner. The error bars in these figures denote the standard deviation for batch-averaged values. The data for large  $N$  are found to obey the empirical equations

$$\langle R^2 \rangle = aN^b \quad (9)$$

and

$$\langle S^2 \rangle = lN^m \quad (10)$$

The solid lines in Figures 3 and 4 represent the least-squares fit of eq 9 and 10 to the data for  $N \geq 20$ . The broken lines are not the fits for  $\langle R_0^2 \rangle^*$  and  $\langle S_0^2 \rangle^*$ , but denote the results obtained by the exact evaluation mentioned above, i.e.,  $\langle R_0^2 \rangle$  and  $\langle S_0^2 \rangle$ . It should be noted that  $\langle R_0^2 \rangle^*$  and  $\langle S_0^2 \rangle^*$  calculated for a finite number of samples by the Monte Carlo method were in good agreement with  $\langle R_0^2 \rangle$  and  $\langle S_0^2 \rangle$  from an exact calculation. The parameters  $a$ ,  $b$ ,  $m$ , and  $l$  analyzed by using eq 9 and 10 for non-self-intersecting chains and the corresponding parameters for unperturbed chains by the Monte Carlo method and by exact calculation are tabulated in Table V. In every case, the data used in analyses are those for  $N \geq 20$ , since they deviated from a linear relation for  $N < 20$ .

The values of  $b$  and  $m$  for unperturbed chains are very close to, though they deviate slightly from, unity. This means that the unperturbed dimensions also deviate slightly from a linear dependence on  $N$  in the region of  $N \leq 151$ . With the interdependent polypeptide model, the unperturbed dimensions

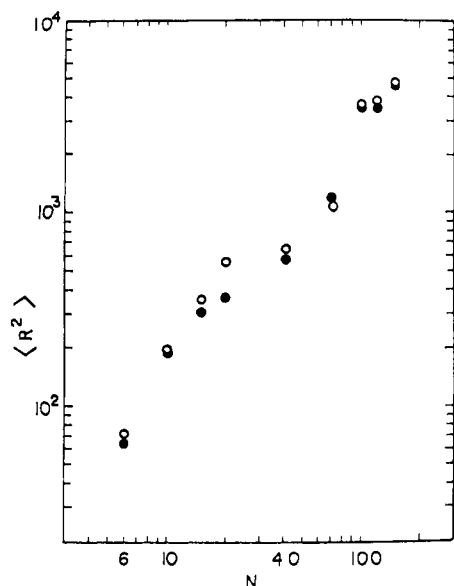


Figure 6. Plots of  $\log \langle R^2 \rangle_{V,D}$  (○) and  $\log \langle R^2 \rangle_V$  (●) against  $\log N$ .

$\langle R_0^2 \rangle$  and  $\langle S_0^2 \rangle$  are almost proportional<sup>2,5</sup> to  $N$  in the range  $N > 200$ . The values of  $a$  obtained both in the present work and in the paper of Knaell and Scott<sup>24</sup> are considerably smaller than 121, the value calculated from the characteristic ratio based on the conformational energy for alanyl dipeptide.<sup>7</sup> As described in the previous section, however, a model effectively equivalent to this dipeptide model can be produced by taking into consideration an appropriate statistical weight for each allowed conformational state. Our value  $b$  for the non-self-intersecting chain model is in good agreement with the value ( $b = 1.20$ ) predicted theoretically for chains with excluded-volume effects,<sup>29</sup> and also with the values (1.18–1.201) obtained from the Monte Carlo calculations for a tetrahedral lattice.<sup>18</sup> Our value of  $m$  is slightly higher than  $b$ , and is in accord with those of other authors.<sup>16, 20, 24</sup> Our values  $a$ ,  $b$ ,  $l$ , and  $m$ , in particular  $m$ , are appreciably different from those of Knaell and Scott<sup>24</sup> based on the same polypeptide model, while they are rather similar to those obtained from the tetrahedral lattice model. This result is mainly attributable to the fact that these two models are different both in conformational state and in the contact distance of atomic pairs. Moreover, it is probable that our three-state model having  $\alpha_L$ ,  $\alpha_R$ , and the extended form resembles the tetrahedral lattice model consisting of *trans*, *gauche*, and the other *gauche*. However, this is not true in general because the amide groups are always fixed in *trans* conformation in our chain model.

(29) S. F. Edwards, *Proc. Phys. Soc. (London)*, **85**, 613 (1965).

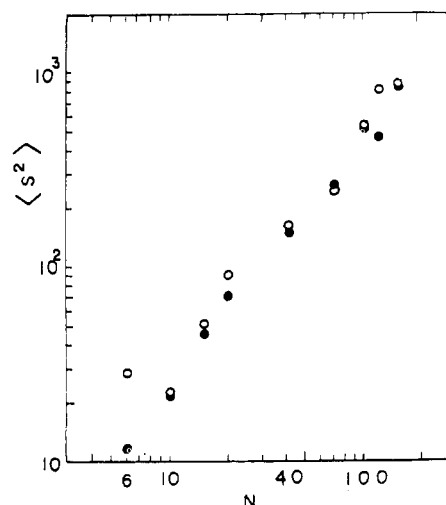


Figure 7. Plots of  $\log \langle S^2 \rangle_{V,D}$  (○) and  $\log \langle S^2 \rangle_V$  (●) against  $\log N$ .

The ratio  $\langle S^2 \rangle / \langle R^2 \rangle$  for the tetrahedral lattice model is 0.157 as opposed to 0.167 for unperturbed chains with infinite chain length. In the off-lattice model of Loftus and Gans,<sup>20</sup> values 0.155–0.153 were obtained. Our results on  $\langle R^2 \rangle_H / \langle S^2 \rangle_H$  and  $\langle R_0^2 \rangle^* / \langle S_0^2 \rangle^*$  directly obtained from the Monte Carlo calculation are shown in Figure 5. The ratios  $\langle R_0^2 \rangle^* / \langle S_0^2 \rangle^*$ ,  $\langle R^2 \rangle / \langle S^2 \rangle$ , and  $\langle R^2 \rangle / \langle S^2 \rangle$  can be derived from Table V. These ratios were found to be practically independent of  $N$ , though dependence on  $N$  was found for non-self-intersecting chains. In these respects, our results differ from those of Knaell and Scott.<sup>24</sup>

By taking into account the conformational energy, we obtained  $\langle R^2 \rangle_{V,D}$  and  $\langle R^2 \rangle_V$  from eq 7.  $\log \langle R^2 \rangle_{V,D}$  and  $\log \langle R^2 \rangle_V$  are plotted against  $\log N$  in Figure 6. In Figure 7,  $\log \langle S^2 \rangle_{V,D}$  and  $\log \langle S^2 \rangle_V$  are plotted against  $\log N$ . As seen from these figures, the dipole interaction decreases  $\langle R^2 \rangle$  and  $\langle S^2 \rangle$  except for  $N = 71$ . Such behavior is in contrast to the effect of dipole interaction on unperturbed dimensions with the dipeptide model.<sup>5</sup> Unfortunately, these data were so scattered that we could not quantitatively discuss them. These quantities are very sensitive to the conformational energy of chains generated. In an extreme case only one chain having the lowest energy among all chains (500–600 in this study) generated contributes to the final result obtained from eq 7, while contributions from other chains have been energetically neglected. In order to obtain more quantitative results according to this method, it is necessary to improve our chain model and calculation method in order to obtain samples having uniform conformational energy. Thus, further studies have to be carried out along these lines before quantitative conclusions can be drawn.